

An FE Simulation Tool For Fracture Mechanics

R. Chandwani, C.M. Timbrell, M. Wiehahn

Zentech International Limited
103 Mytchett Road
Camberley
Surrey
GU16 6ES
U.K.
<http://www.zentech.co.uk>

ABSTRACT

The use of fracture mechanics techniques in the assessment of performance and reliability of structures is on the increase and the prediction of crack propagation of an existing or postulated flaw in a structure plays an important part. A software simulation tool, which uses FEA, has been developed to quantitatively predict the propagation of 3D non-planar cracks through structures. This tool allows calculation of stress intensity factors and energy release rates and can be applied in a variety of commercially important applications. These include design of laboratory experiments, testing and developing advanced materials, assessing the effects of surface treatments and the study of component repairs.

INTRODUCTION

Fracture mechanics is the science of predicting the behaviour of material in the presence of flaws or cracks. Such flaws may be the result, for example, of manufacturing processes or they may initiate over time as the result of in-service loading. Once present, cracks may propagate as a result of time dependent load effects or due to cyclic loading.

Structures designed “correctly” from static load considerations may not reach design life because of the effect of crack propagation. This is a major issue in a variety of industries in which damage tolerance is a key part of the design process. Aerospace structures, gas turbine engines, pressure vessels and pipelines are obvious examples where failure could lead to catastrophic consequences and loss of life.

Increasing demands of reliability and performance mean that the often over conservative empirical methods in codes of practice can produce less than optimised designs. On-going safety assessment for in-service components requires the prediction of future crack growth rates.

In addition to these well recognised areas for crack growth simulation, the on-going software and hardware developments make possible new areas of investigation. These include:

- Design of experiments
- Combining numerical analysis with experimental testing and material development
- Studying composite patch repairs
- Studying the effect of surface treatment
- Studying interfacial cracks

Zentech has developed a 3D crack analysis tool called ZENCRACK (Ref. 1). ZENCRACK reads in an uncracked finite element model and produces a cracked finite element model. Stress intensity factors or the energy release rate are calculated automatically from the results of the cracked finite element analysis. Furthermore crack growth can be undertaken by extending the crack position. An updated finite element model is then created and run to simulate crack growth. ZENCRACK is a mature product that was first released in 1990.

TOPOLOGICAL ISSUES

A critical issue that must be addressed in 3D F.E. fracture mechanics analysis is that of mesh generation. In the simplest of geometric cases where symmetry can be used, it may be possible to utilise standard mesh generation tools to produce a crack of the required size. In the general case, however, the use of standard tools poses several time consuming problems including:

- Component geometries are often complex and time consuming to model in their uncracked forms.
- Defects often occur at geometrically difficult locations e.g. corners, welds, chamfers.
- Initial cracks of the correct size and shape must be inserted into the component at the correct location.
- Cracks may develop in a non-planar fashion depending upon the loading.
- These problems are compounded if more than one crack size must be analysed or if there are multiple cracks in a component.

The approach that has been successfully adopted at Zentech is the use of 'crack-blocks' which model the details of the crack region. Figure 1 and Figure 2 demonstrate the use of the crack-block methodology in generating a cracked mesh from a user-supplied intact component. The method works by replacing one or more elements in the uncracked mesh by crack-blocks that contain sections of crack front.

ZENCRACK has two types of crack-blocks:

- **Standard crack-blocks.**
 - These crack-blocks have a "clean" face on three faces.
 - The crack-blocks are designed to replace elements in the mesh by updating element connectivities and node numbers (see Figure 1).
 - The crack-blocks consist of "through" and "quarter circular" crack-blocks.
- **Large crack-blocks.**
 - These crack-blocks do not have "clean" faces.
 - These crack-blocks use tied contact to tie the crack-blocks to the model and can therefore straddle several standard elements (see Figure 2).
 - The crack-blocks consist of "through" and "quarter circular" crack-blocks.

The crack-blocks have a varying number of "rings" of elements around the crack front. The innermost ring contains "collapsed" elements to represent the singularity in the stress and strain field at the crack front. ZENCRACK offers full control of the nodes along the crack front and the radial nodes closest to the crack front in order to generate a singularity best suited to LEFM or EPFM (Ref. 2).

Although the crack-blocks are referenced as "quarter circular" or "through" crack-blocks, the user has control of the initial crack front shape which may be defined by fitting a spline through a series of points for the greatest flexibility in definition.

Loading (e.g. pressure load) and boundary conditions are updated as the crack-blocks are incorporated into a mesh.

By processing fracture mechanics parameters from a cracked mesh and adding a crack growth algorithm, it is possible to carry out automatic crack growth prediction, as summarised in Figure 3.

This introduces a number of additional challenges. In order to obtain best results from the mesh within the crack-blocks, their outer boundaries must be manipulated to reduce internal element distortion as much as possible. Further, to allow a crack to develop through a model, it must be possible to allow crack-blocks to transfer from one position to another. This requires manipulation of the elements outside the crack-blocks, again to reduce distortion in the mesh. These methods are shown for a side view of a cracked mesh in Figure 4.

It must be made clear that there is no single method of crack modelling and re-meshing that can be used for all crack geometries. However, the combination of standard and large crack-blocks in conjunction with mesh manipulation algorithms, allows many difficult problems to be addressed in a timely fashion.

FRACTURE MECHANICS PARAMETERS

The primary fracture mechanics parameters that may be of interest for crack propagation are:

- Stress intensity factors, K_I , K_{II} , K_{III}
- Energy release rate, G

The stress intensity factor approach was developed by Irwin in the 1950s following on from the elastic strain energy approach to brittle fracture developed by Griffith from the 1920s. Irwin's work led to the foundations for the concept of linear elastic fracture mechanics (LEFM) which is still fundamental in most crack propagation analyses.

For linear elastic analysis the concepts of energy release rate and stress intensity factors are closely linked. The stress intensity factors describe the magnitude of the elastic stress field at a crack front. The general form of the stress intensity factor is:

$$K = f(\text{load}, \text{crack length}, \text{geometry}) \quad \text{Equation 1}$$

For mode I behaviour it can be shown that:

$$K = \left(\frac{EG}{1 - (\alpha\nu)^2} \right)^{1/2} \quad \text{Equation 2}$$

where E is Young's modulus, ν is the Poisson ratio and α is a value ranging from 0 for plane stress to 1 for plane strain. In a more general form it is possible to write:

$$G = \frac{B}{E} (K_I^2 + K_{II}^2) + \left(\frac{1+\nu}{E} \right) K_{III}^2 \quad \text{Equation 3}$$

where $B=1$ for plane stress and $1-\nu^2$ for plane strain.

Another important relationship for stress intensity factors in linear elastic analysis is based on the Westergaard equations that link the stress intensity factors to the displacement field around the crack tip (COD) giving:

$$K_I = \frac{EV_i}{4B} \sqrt{\frac{2\pi}{r}}, \quad K_{II} = \frac{EV_{ii}}{4B} \sqrt{\frac{2\pi}{r}}, \quad K_{III} = \frac{E}{2(1+\nu)} V_{iii} \sqrt{\frac{\pi}{2r}} \quad \text{Equation 4}$$

where B is defined as above and V_i , V_{ii} and V_{iii} are the relative opening displacements at a radius r from the crack front for an orthogonal system aligned with the mode I, II and III directions. This approach is widely used by practitioners of both the finite element and boundary element methods and has the benefit that it requires relatively little additional effort on top of the basic stress solution. The drawback to the method is that it requires a state of stress assumption.

Calculation of the magnitudes of energy release rate and / or stress intensity factors do not directly provide directional information regarding crack growth. A number of criteria have been developed to specify the direction. They include maximum energy release rate, maximum tangential stress and the normal to the maximum principal stress. In the context of numerical calculations of energy release rate and stress intensity factor, the two most useful criteria are maximum energy release rate and a direction based on stress intensity factors e.g. maximum tangential stress criterion:

$$\theta = \cos^{-1} \left(\frac{3K_{II}^2 + \sqrt{K_I^4 + 8K_I^2 K_{II}^2}}{K_I^2 + 9K_{II}^2} \right) \quad \text{Equation 5}$$

The J-integral concept was first described by Rice in the late 1960s. It is an energy based concept in which the J-integral, J , can be considered a non-linear elastic equivalent of the energy release rate, G . By definition G and J are the same for elastic behaviour. The J-integral can be calculated from specific procedures within some finite element codes (e.g. *CONTOUR INTEGRAL in Abaqus/Standard, FRACTURE in Finas, LORENZI in MSC.Marc). In order to calculate the maximum energy release rate magnitude and direction at a crack front node, several evaluations of energy release are calculated for different postulated extensions of the crack front. From the resulting energy values, the maximum can be calculated. This is shown schematically in Figure 5.

CRACK GROWTH PREDICTION

In order to complete the crack growth prediction, it is necessary to integrate using the fracture mechanics parameters from a f.e. analysis along with the crack growth data and a load history. This can be done for simple case only or extended to situations of

more practical interest. In the latter case a number of scenarios must be dealt with. These include:

- Different “load systems” e.g. including effects of
 - Spectral loading and fatigue crack growth
 - Residual stress and static loading
 - Retardation (Willenborg)
 - The 2 points above both have the effect of changing the effective stress ratio e.g. for cyclic and static load:

$$R_{effective} = \frac{K_{cyclic\ min} + K_{static}}{K_{cyclic\ max} + K_{static}}$$

- Time dependent crack growth
- Material data
 - Cyclic crack growth data, da/dn vs ΔK
 - Simple forms, e.g. Paris, Walker
 - Tabular data as a function for R, temperature
 - User subroutine for proprietary models
 - Time dependent crack growth data, da/dt vs K
 - Options to include temperature dependency
 - Threshold
 - Fracture

Fatigue crack growth can occur under constant amplitude cyclic loading or, more commonly in practical cases, as a result of load levels that vary randomly with time. In order to use this type of time series loading for fatigue crack growth calculations, it must first be converted into a cycle counted spectrum. This is most often performed with the rainflow counting technique. The result of this count is a load spectrum in which each cycle has a specified minimum and maximum load level. The stress ratio for the cycle is the ratio of the minimum to maximum loads, denoted as R. In general each cycle may differ from the next in either minimum or maximum load level or both. In particular cases, however, there may be blocks of consecutive cycles of the same stress ratio.

The basic load-time data and the counted cyclic load data are the fundamental load history inputs for time dependent and fatigue crack growth calculations respectively.

Handling complex load histories

In order to tackle different types of fatigue and time dependent loading within an integration scheme, a number of basic load system types are defined:

- Static system (i.e. no cyclic effects)
 - e.g. residual stress or centrifugal load
- Constant amplitude system
 - Single stress ratio
- Spectrum system
 - Multiple load blocks of min., max. load, # cycles
- Minimum system

- References a load step in the f.e. analysis that includes a static load plus minimum cyclic load
- Maximum system
 - References a load step in the f.e. analysis that includes a static load plus maximum cyclic load
- Superposition system
 - Combination of a static and cyclic system, or,
 - Combination of a minimum and maximum system

The basic load systems are set up for fatigue analysis. However, time dependent loading can be added into a static, constant amplitude or cyclic system. Load systems can be combined in sequence to generate a complete load spectrum.

When fatigue-only analysis is carried out, the loading must be of a cyclic nature. Load time histories and temperature time histories are not relevant although spatial temperature distributions along the crack front are allowed and mean that temperature dependent material properties can have an effect on growth calculations. The loading is grouped into “blocks” of cycles each containing one or more cycles. Unless there is retardation present the integration scheme is able to attempt integration to the end of each block in turn.

When time-only analysis is carried out, the loading is defined in terms of a series of load values at particular times i.e. a load time history. The load is assumed to vary linearly from one load level to the next. This type of load time history must be defined via a load time history file. The integration takes each segment in turn (i.e. each line segment between successive pairs of points) and calculates the da for the segment. Temperature time history may also be included in this type of analysis. An example of a load-time history is shown in Figure 6.

When combined fatigue and time dependent analysis is carried out, the loading consists of a load time history and cyclic spectrum data that includes time information. This time information allows each load cycle to be positioned within the timeline, as shown in Figure 7. The integration proceeds in a similar fashion to a time dependent integration with the complication that the fatigue effect of each cycle must be added instantaneously when the time for the cycle is reached. Temperature time history may also be included in this type of analysis.

The load systems must be cross-referenced to load steps within the finite element analysis. These load steps provide fracture mechanics parameters for a given load level. During the integration the parameters are scaled and updated as necessary to account for the “current” load levels within the load spectrum.

- The number of unique load conditions is identified and an analysis step is set up for each load condition in the finite element model (e.g. tension and bending as two load conditions).
- For a given crack size this provides:
 - One crack front stress state for each load condition.
 - One set of energy release rate and displacement data for each load condition.

- A number of load systems are defined each of which is based on the basic load conditions. A load system may be of type static, constant amplitude, spectrum, minimum or maximum.
- A load system must use the energy release rate data for the appropriate load condition.
- More than one load system may be based on one load condition.
- A superposition load system may be constructed by combining a static and cyclic system or a minimum and maximum load system.
- The total load spectrum is defined by a sequence of load systems.

A schematic example of this process is shown in Figure 8.

Having set out the load systems and cross referencing of results for a crack position from the f.e. analysis, the challenge is to obtain an accurate growth prediction without having to analyse each load cycle separately. The following discussion will consider fatigue crack growth only.

Fatigue crack growth integration

Numerical integration **during** crack advancement is the only method of achieving a valid solution for all types of crack growth data for an arbitrary 3D crack front. For general growth data it is not correct to advance the crack using a simple Paris method in order to generate K vs a data, followed by integration to find the number of cycles at the end of the analysis. Instead a two-pass integration approach is used after each f.e. analysis to obtain correct crack advancement and consistent dN at all nodes on the crack front.

Integration over a large number of cycles requires some assumption about the way that the fracture mechanics parameters will vary over the step. Consider the general form of the stress intensity factor for a given load:

$$K = f(\text{geometry}) \sigma \sqrt{\pi a} \quad \text{Equation 6}$$

Neglecting effects of the geometry function gives an approximation that:

$$K^2 \propto a \quad \text{Equation 7}$$

and therefore using Equation 2:

$$G \propto a \quad \text{Equation 8}$$

So, the simplest approach that the value of K or G is constant over the step will not be very accurate for large steps. A better assumption is that dG/da is constant over the step. The initial and final G values for a given load level can then be expressed as:

$$G_{\max \text{ final}} = G_{\max \text{ initial}} + \left(\frac{dG_{\max}}{da} \right) da \quad \text{Equation 9}$$

This method requires an estimate of dG/da for the next integration step based on history from previous steps.

Numerical integration of the crack growth data incorporating Equation 9 is based on an energy form of the crack growth law:

$$\frac{da}{dN} = g(\Delta\sqrt{G}, R, T, f) \quad \text{Equation 10}$$

This allows a general integral to be written:

$$\int_i^f dN = \int_i^f \frac{1}{g(\Delta\sqrt{G}, R, T, f)} da \quad \text{Equation 11}$$

Due to the fact that there are multiple node positions on the crack front, this integral must be evaluated in a 2-pass process. In the first pass, each node is integrated for the specified value of da for the step and dN is evaluated. In general this produces different dN values for each node. The minimum dN is taken to be the critical value and a second integration pass is carried out in which the da is calculated at every node for this critical dN . This provides a consistent dN calculation and in general different da for each node.

Clearly the choice of the step size, da , is important in this process, as is the method calculation of dG/da . But comparison of the predicted value of G and the actual value of G after the advanced crack has been analysed allows calculation of an error term that is used to control the step size. This is shown schematically in Figure 9.

After a finite element analysis is completed ZENCRACK has an “accurate” value for G at each crack front node. This is denoted by G_{FEi} for the i^{th} finite element analysis. During integration Equation 9 is used to obtain the updated crack front position and at the end of the integration the growth magnitude is da_{FE} and the expected value of G from the next finite element analysis is:

$$G_{ESTIMATEi+1} = G_{FEi} + \left(\frac{dG}{da} \right) da_{FE} \quad \text{Equation 12}$$

When the analysis of the updated crack front is completed, an “accurate” value for G is available for the $i+1^{\text{th}}$ finite element analysis, G_{FEi+1} . As Equation 12 is just an approximation the difference between G_{FEi+1} and $G_{ESTIMATEi+1}$ is an indicator of how accurate the integration was for the last step. This error term is used to control the maximum da for the next integration step. If the error is below a specified tolerance, the step size may increase. Otherwise the step size is reduced. In this way the analysis is controllable based on a quantifiable error term rather than an arbitrary selection of da . There are additional details in the way that this scheme is implemented, but this description provides the basic concept.

Comparison of growth predictions using different assumptions

This section considers growth of a semi-elliptical surface crack in a bar under uni-axial tension. The model for this analysis, plus more background information on the geometry and loading, is given in Figure 4-6 of Ref. 3. A summary is shown in Figure 10. The purpose of this example is to demonstrate the benefit of an error control algorithm over an integration scheme that uses a fixed step. A number of other numerical problems associated with the integration are also discussed.

Without step size adjustment from integration step to the next there is no means to reliably control the stability and accuracy of the analysis. If a fixed step size is assumed, it is not obvious what the size of that step should be. If the step is too small, there will be high number of f.e. analyses. If the step is too large the crack shape may become unstable and the results will be inaccurate.

The method of calculating dG/da can also affect the analysis. For example, consider these four possibilities:

damped method	Use a weighted average dG/da with damping. Damping is applied to the growth and G distributions to reduce potential oscillations building up in the crack front shape. The weighted average is calculated by taking contributions from all nodes including non-growing nodes.
local method	Use a simple local dG/da definition for each crack front node: $dG/da = (G_{new} - G_{old}) / da$
local averaged method	Use a local dG/da definition for each crack front node: $(dG/da)_{new} = (G_{new} - G_{old}) / da$. Then average the dG/da value with the previous value: $dG/da = [(dG/da)_{new} + (dG/da)_{old}] / 2$.
average method	Use an average dG/da definition for each crack front node: $dG/da = \text{sum of } [(G_{new} - G_{old}) / da] / \text{number of nodes on crack front}$. This average is calculated by taking contributions only from nodes that are growing, all of which will have the same dG/da . All non-growing nodes have $dG/da=0$.

It is not clear from these definitions which may be the best to use. Experience shows that in the majority of cases the damped method produces the most stable solution. For certain classes of problem, the local averaged method is better e.g. when some of the crack front is below threshold, or for superposition of static and cyclic load systems.

Figure 11 compares the results of analyses that use fixed stepping and a “poor” choice of dG/da against error control stepping and a “good” choice of dG/da calculation. The growth profiles for the fixed step analysis show severe oscillations. This is due to a combination of the fixed step size being too large and the choice of method for evaluating dG/da . The error control solution, on the other hand, shows

smooth profiles that are gradually increasing in separation. This is due to the increase in the step size that is allowed because the error on the G term is within tolerance.

Figure 12 shows the results in the depth direction in terms of K vs a and a vs N. For the fixed step analysis with profile oscillation there is a marked saw-tooth effect in the K vs a plot. This manifests itself in an inaccurate life prediction. The error control analysis on the other hand, appears to have given a smooth, valid and accurate solution.

Figure 13 shows the results of investigation of the initial step size on the accuracy of the solution. A fixed step analysis with a very small step of 0.05mm has been analysed to produce a “target” solution. This required 747 finite element analyses, which is clearly far too many for practical situations. However, it demonstrates that as the fixed step size is increased to 0.75mm, 1.5mm and 3.0mm there is divergence from the target solution. The 0.75mm step requires 51 f.e. analyses and produces an equally accurate result as the 0.05mm analysis. The 1.5mm and 3.0mm analyses, whilst taking less f.e. steps (27 and 17 respectively), show a reduction in the predicted life.

The analyses with error control on Figure 13 have initial step sizes of 0.75mm, 1.5mm and 3.0mm and have been run with a default value of 2% allowed error on the G term. The way the error control scheme works is to cut-back the step size during the first few steps in order to capture the important region of start-up where a small amount of crack growth can be due to large numbers of cycles:

$$\text{daTOLstep} = \text{TOLa} \times (\text{FE number} / \text{nFEscale})^{\text{factorFEscale}}$$

where by TOLa is the value defined as the “initial” step size and by default nFEscale=10 and factorFEscale=3 (i.e. cut-backs occur over the first 10 f.e. analyses with a power of 3).

If the tolerance is exceeded during this cut-back period, the cut-back is de-activated and the step size is controlled purely on the tolerance limit. It can be seen that the choice of initial step size has had little effect on the results, all of which show good agreement with the target solution. The number of f.e steps varies between 29 and 37. It is noted that the error control analysis with 29 steps gives significantly better agreement with the target solution than the fixed step analysis with 27 steps.

The effect of the error tolerance and the severity of the start-up cutbacks is investigated in Figure 14. Analyses with 2%, 5% and 10% error control and less severe cut-backs (power=2 rather than 3) all give similar results for similar numbers of f.e. steps.

The error control scheme is considered to be both efficient and accurate in integration for life prediction.

SAMPLE APPLICATIONS

It is not possible to give details of all applications that these methods have been used on, partly because of commercial confidence. However, successful applications include:

- Non-planar growth simulation and life prediction in an aero engine nozzle guide vane.
- Power plant thermo mechanical fatigue crack growth combined with time dependent crack growth.
- Stress intensity factor determination for gas transmission pipelines.
- Composite patch repairs in welded structures.
- Assessment of damage associated with flaws at unknown locations, through the combined use of analytical models and measured vibration signatures (Ref. 4).
- Determination of interfacial toughness curves (Ref. 5).

EXAMPLES OF CRACK GROWTH

Some of the crack growth capabilities of ZENCRACK are shown in three examples:

- A SEN specimen with residual stress and cyclic external load.
- A 43° oblique crack.
- Non-planar growth in a specimen with a hole.

It must be noted that each analysis, once started, is completed fully automatically.

The first example shows a straightforward geometry – a simple model of a SEN specimen (Figure 15). The loading, however, is combined residual stress and cyclic external load. The structural steel used in the specimens had a yield stress of 330MPa and a tensile strength of 510MPa. The plate specimens were originally 200mm by 70mm by 10mm thick, welded along the longitudinal centreline by electron beam welding which generated a symmetric distribution of residual stress about this line having a magnitude of about 330MPa (tension) at the centre and about 40MPa (compression) at the two edges, the tensile region extending to about 10mm on both sides of the centreline. After welding, the thickness of the welded specimen was reduced to 6mm by shaping and fine grinding both surfaces in order to minimize the variation of the residual stress through the thickness of the specimen. The initial crack depth is 10mm. The external load is a cyclic load varying between 0 and 150MPa. Due to the combination of static and cyclic loading the effective stress ratio will vary and crack growth data is a function of R (Figure 16). Further information is available in the original references by Kang et al (Ref. 6, Ref. 7). The model has been analysed with $\nu=0$ to allow comparison with AFGROW (Ref. 8).

The stress intensity factors for the maximum external load and the residual stress distribution are compared in Figure 17 and Figure 18 with reference results. The agreement is clearly very good. Comparisons of crack growth simulations by ZENCRACK and AFGROW are shown in Figure 19 and Figure 20 for cases with

external load only and external load plus the residual stress respectively. Again there is good agreement and the effect of the compressive residual stress is seen in an increase of life by a factor of around 5. Further information on these results, plus additional cases, is available in Ref. 9.

The second example is of a 43 degree slanting crack in a plate under cyclic axial tension (see Figure 21). This is based on a test case for which experimental data is published (Ref. 10). The crack face triangular facets that are defined by ZENCRACK for the initial crack, plus those calculated during the analysis, are shown in Figure 22 with Mises stress plots at two stages of the analysis shown in Figure 23. The growth is compared against experimental results in Figure 24 and Figure 25. It is clear that there is excellent agreement in both the calculated growth direction and cycle history. Note that although the problem is initially mixed mode, the crack very quickly re-aligns itself into mode I behaviour.

The third example is a 4-point bend specimen containing a circular hole and a through thickness crack. This is based on a test case for which experimental data is published in Ref. 11. The reference also contains a 2D plane strain calculation of the crack path. For this example it is possible to compare the crack paths but not the cycle count (due to insufficient details available in the reference).

The top picture in Figure 26 shows the uncracked model with the offset hole. The remaining pictures show the initial through thickness crack and the meshing at three stages during the growth prediction. This example shows how the crack-blocks are rotated to try to keep them sensibly aligned with the crack front, whilst the surrounding elements are relaxed. It is clear that a significant amount of element shifting and relaxation is required to complete this analysis. Figure 27 shows the agreement between the ZENCRACK prediction and the reference.

CONCLUSIONS

A general crack growth scheme has been successfully implemented in ZENCRACK. It allows crack advancement and non-planar crack growth simulation in 3D finite element models. For fatigue crack growth simulations a full thermo mechanical implementation is available. For time dependent crack growth simulations a load and temperature time history can be specified. In addition, the effects of fatigue and time dependent growth may be analysed in a single analysis.

REFERENCES

- Ref. 1 ZENCRACK
Zentech International Limited, U.K.
<http://www.zentech.co.uk/zencrack.htm>
- Ref. 2 “Use of modified standard 20-node isoparametric brick elements for representing stress/strain fields at a crack tip for elastic and perfectly plastic material”, Koers,R.W.J., Int. J. Frac. 40 (1979) 79-110.
- Ref. 3 ZENCRACK 7.3 Examples Manual
Zentech International Limited, U.K.
<http://www.zentech.co.uk/zencrack.htm>
- Ref. 4 “Simulation Of Deformation Modes For Damage Detection In Turbine Engine Disks”, R. Brockman, R. John, Materials Science & Technology 2004 Conference & Exhibition, New Orleans, Louisiana, USA, September 26–29, 2004.
- Ref. 5 “Determination of interfacial toughness curves using experiments and simulations”, F. Leblanc, J. Roger, A.Zimmermann, D.Coutellier, Journées Nationales sur les Composites #14, UTC, Compiègne, France, 22-24 March 2005.
- Ref. 6 “Fatigue Crack Growth and Closure Behavior through a Compressive Residual Stress Field”, Kang, K.J., Song, J.H. and Earmme, Y.Y., Fatigue Fracture Engineering Mater. Struct. Vol.13, No.1, pp. 1-13, 1990.
- Ref. 7 “Fatigue Crack Growth and Closure through a Tensile Residual Stress Field under Compressive Applied Loading”, Kang, K.J., Song, J.H. and Earmme, Y.Y., Fatigue Fracture Engineering Mater. Struct. Vol.12, No.5, pp. 363-376, 1989.
- Ref. 8 AFGROW,
Air Vehicles Directorate, Air Force Research Laboratory, U.S.A.
<http://afgrow.wpafb.af.mil/>
- Ref. 9 “Improved life prediction of turbine engine components using a finite element based software called ZENCRACK,” SBIR Phase II (f33615-01-c-5211), Sponsoring Agency: Materials and Manufacturing Directorate, Air Force Research Laboratory, Wright-Patterson AFB, OH 45433-7817, USA.
- Ref. 10 “Fatigue crack propagation under general in-plane loading - I: Experiments”, M.A. Pustejovsky, Engineering Fracture Mechanics 11 (1979) 9-15.
- Ref. 11 “Fatigue life and crack path predictions in generic 2D structural components”, A.C.O. Miranda, M.A. Meggiolaro, J.T.P. Castro, L.F. Martha, T.N. Bittencourt, Engineering Fracture Mechanics 70 (2003) 1259-1279.

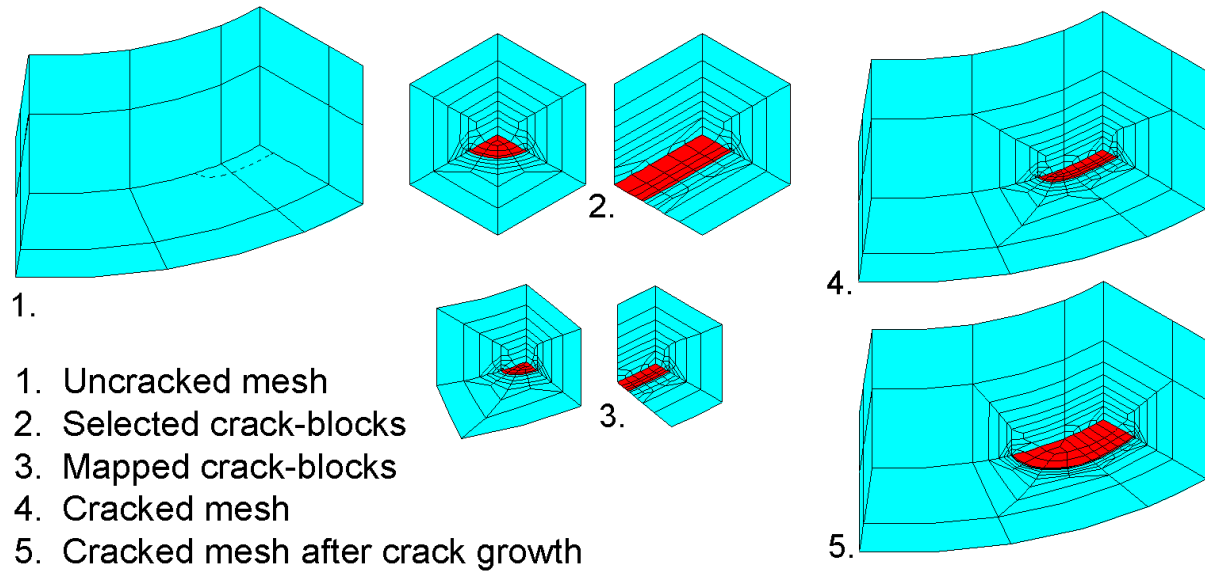
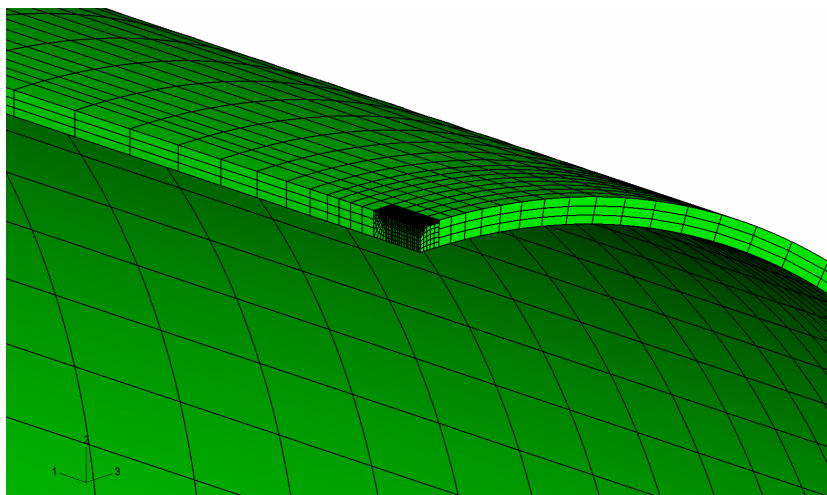
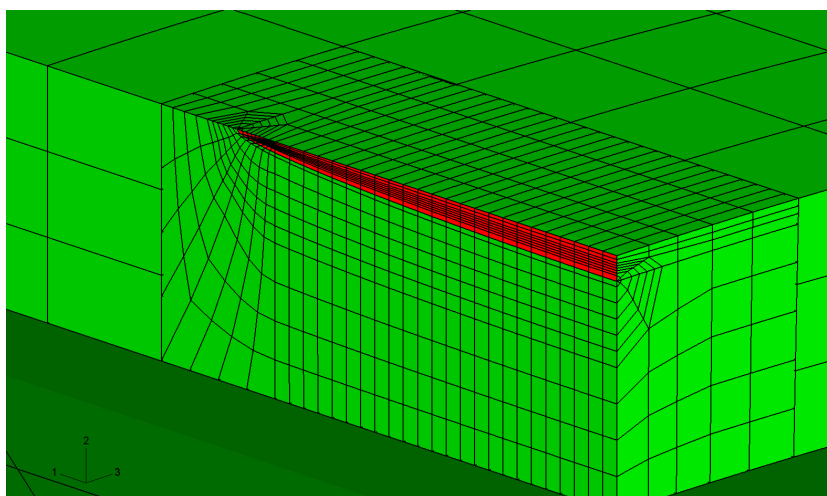


Figure 1 - Summary of crack insertion and mesh update process using standard crack-blocks



10% outer wall crack with aspect ratio 1:20 in a 1/2" thick gas transmission pipeline with outer diameter 36".



Close-up of the above view showing the large crack-blocks surrounded by the mesh. Surface based tying is used across the dis-similar interface of the two mesh regions.

Figure 2 - Example of large crack-blocks

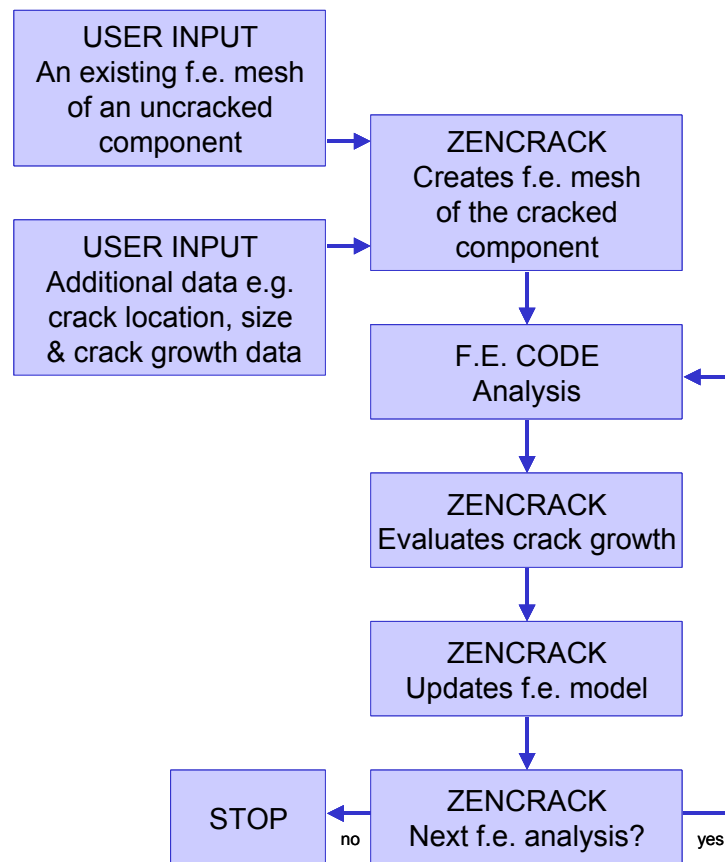


Figure 3 - Simplified flow chart for crack growth prediction analysis

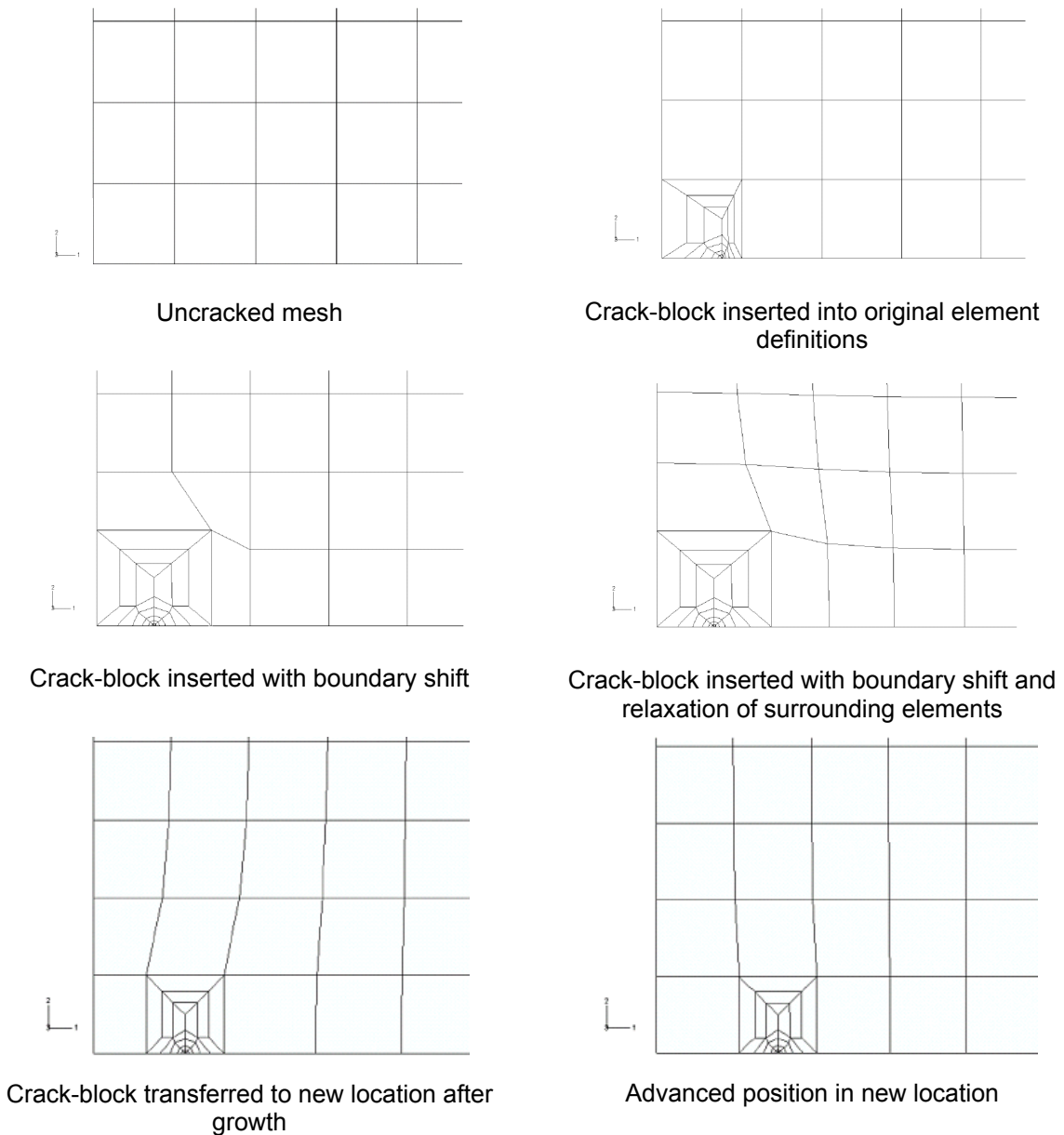


Figure 4 - Demonstration of boundary shifting, relaxation and crack-block transfer

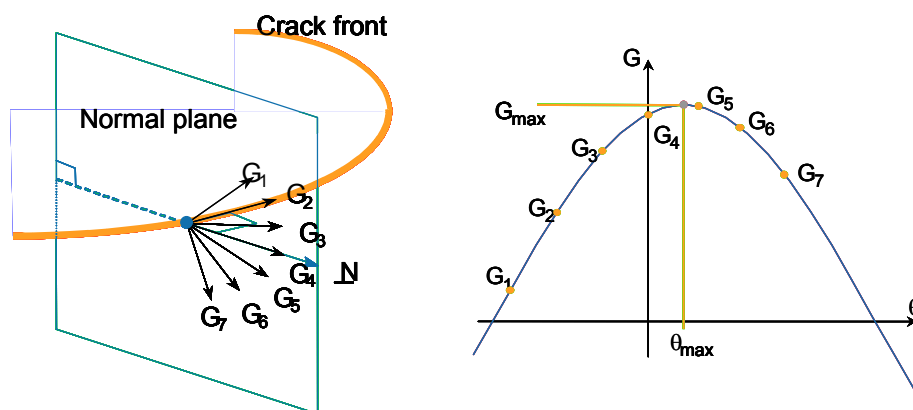


Figure 5 – Energy based calculation of G_{max} and growth direction

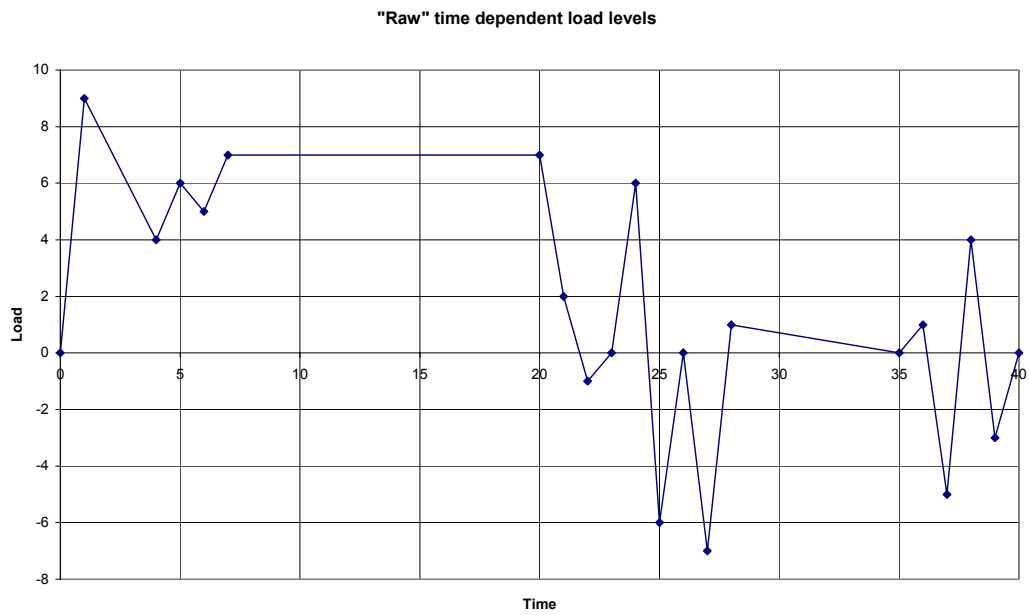


Figure 6 – Load time history

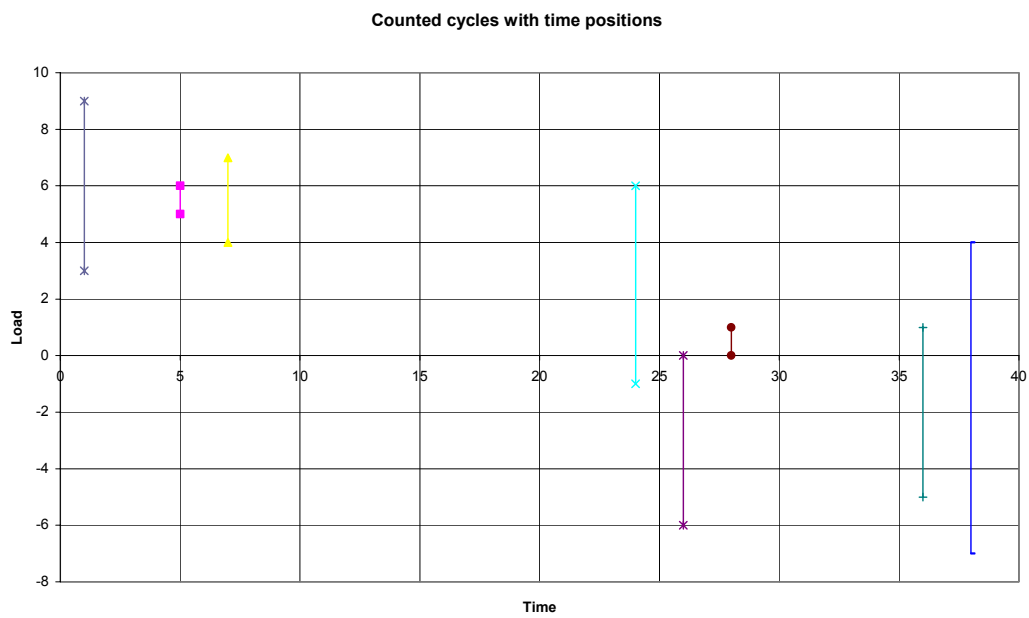
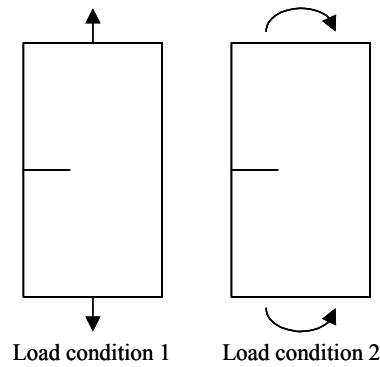
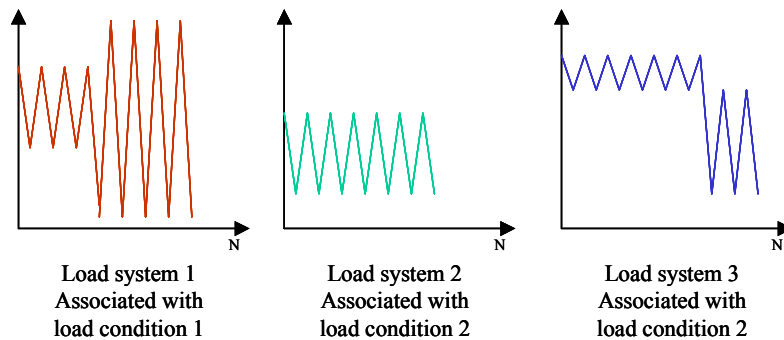
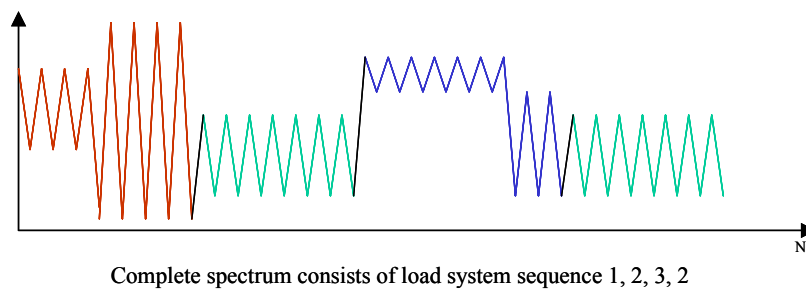
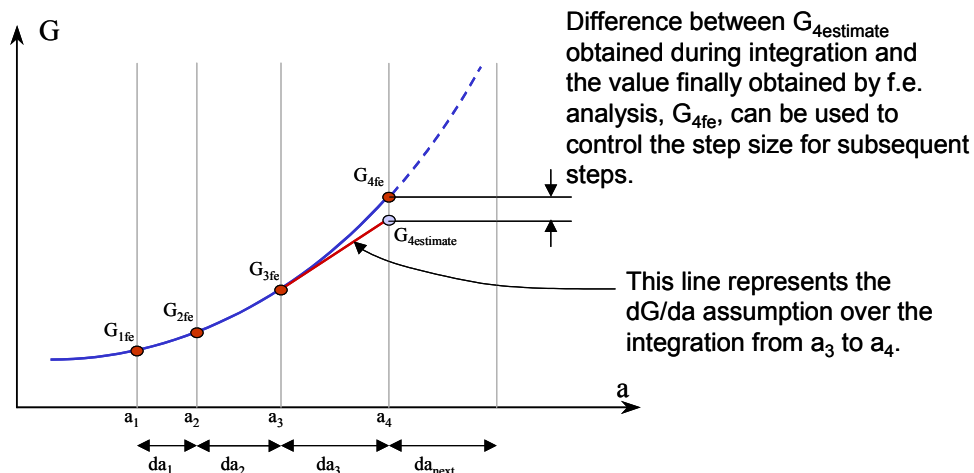


Figure 7 – Counted fatigue spectrum with cycles at known time points

Load Conditions**Load Systems****Load Spectrum****Figure 8 – Example of associating load conditions with cyclic load systems****Figure 9 – Potential error in G when using a constant dG/da assumption**

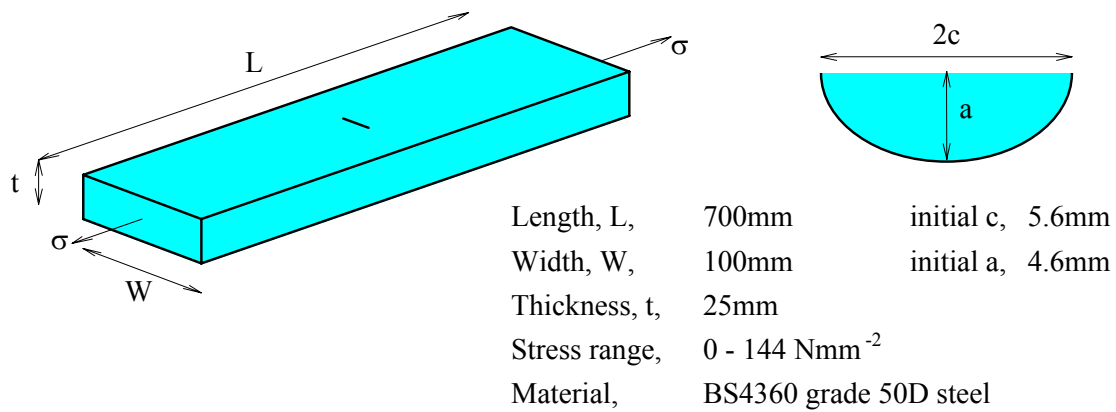
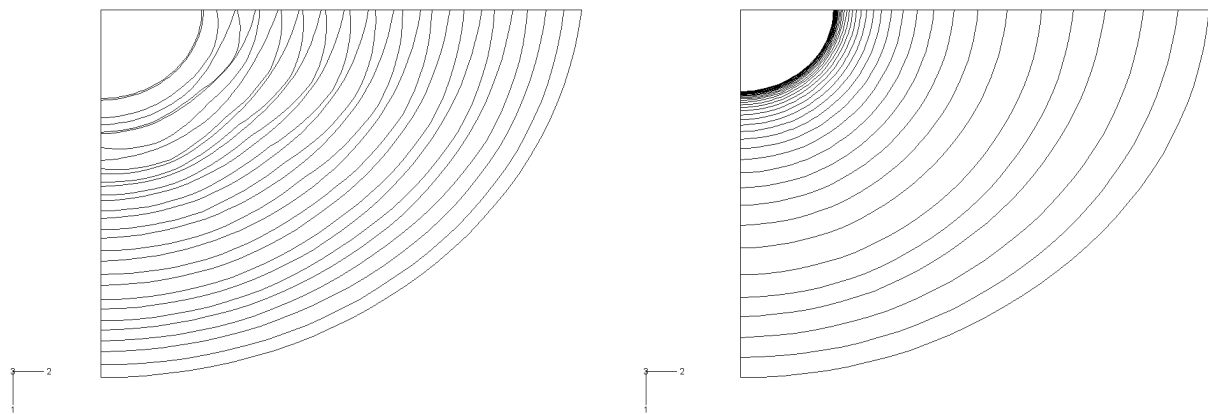


Figure 10 – Geometry for example problem



Analysis with oscillations in profiles: resulting from use of fixed step algorithm and non-default dG/da evaluation

Analysis without oscillations in profiles: resulting from error control algorithm and default dG/da evaluation

Figure 11 – Oscillations in a crack front profiles

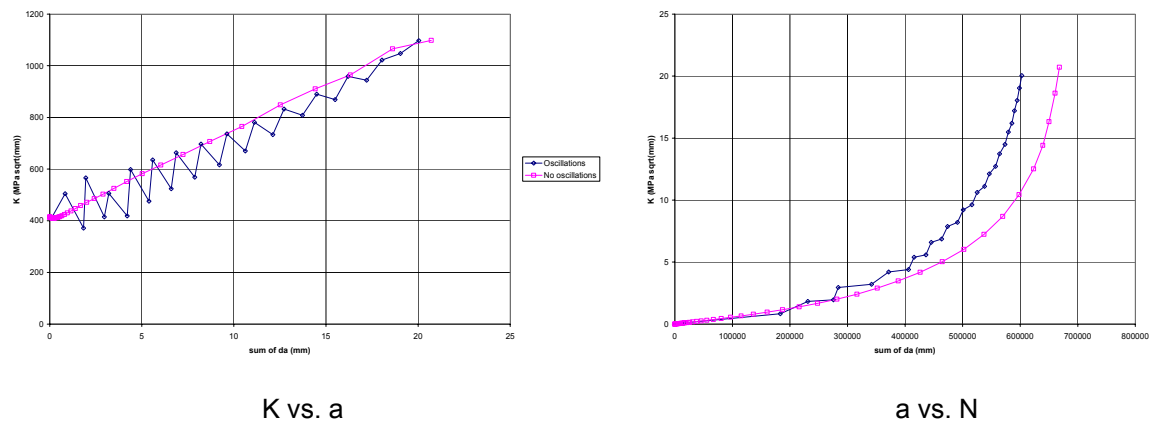


Figure 12 – Results with and without oscillations in crack front profiles

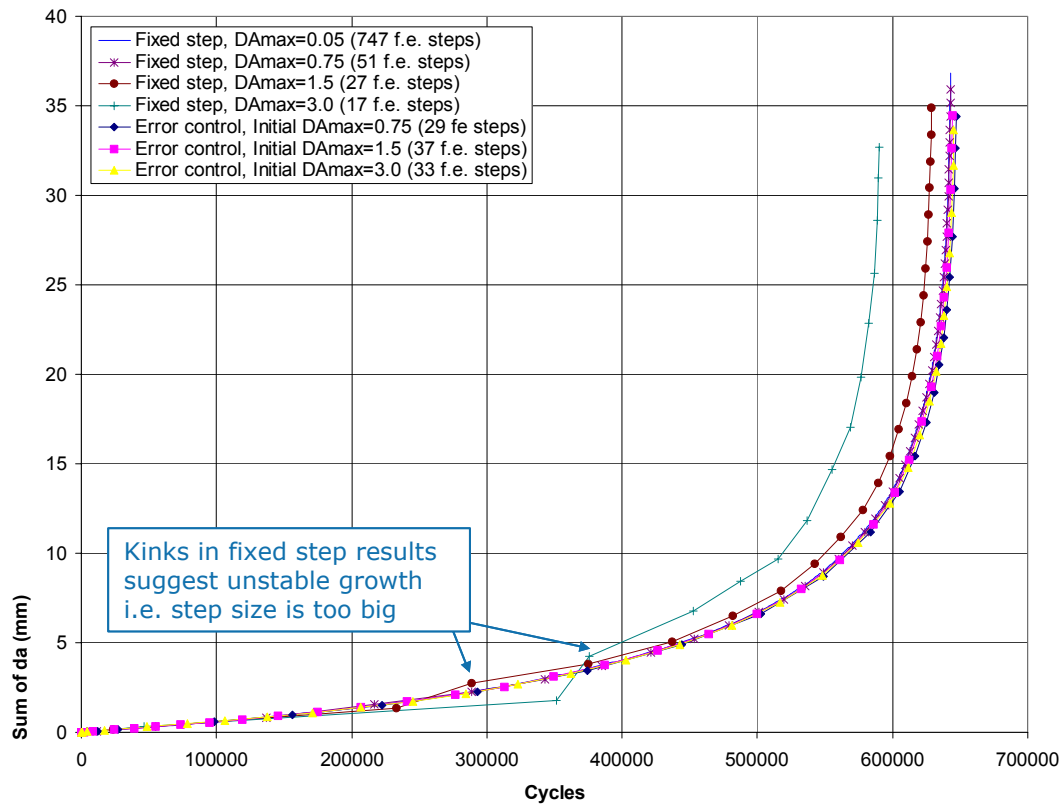


Figure 13 – Comparison of fixed step and error control step

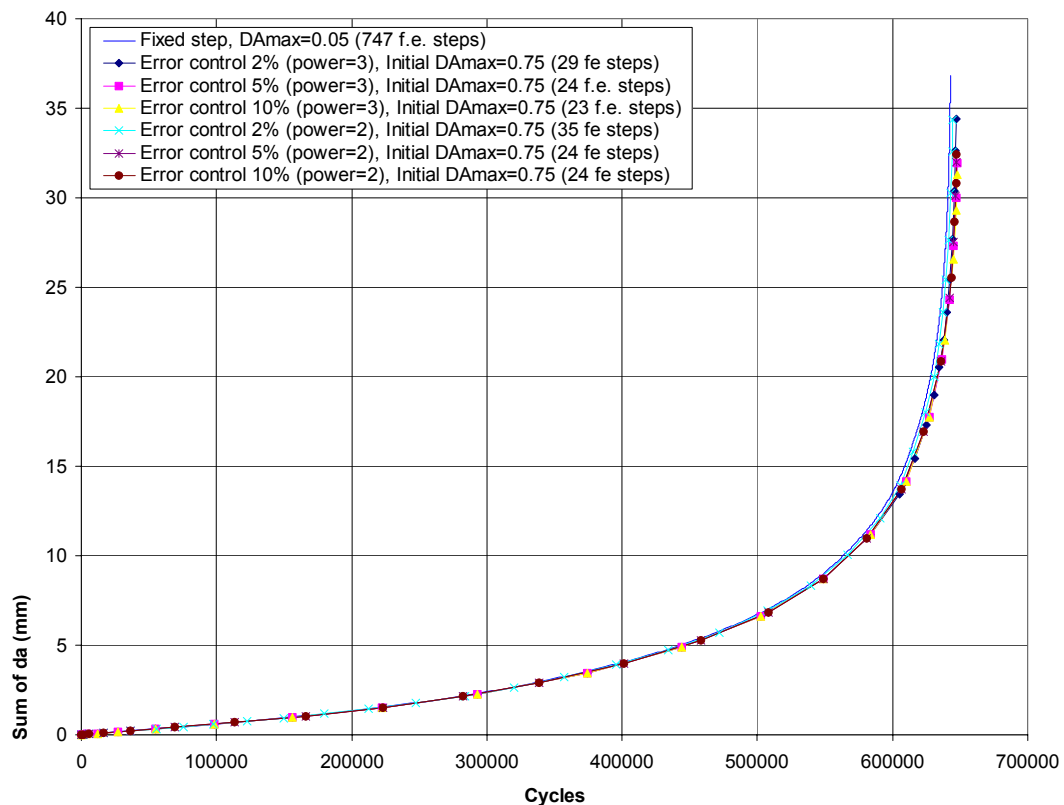
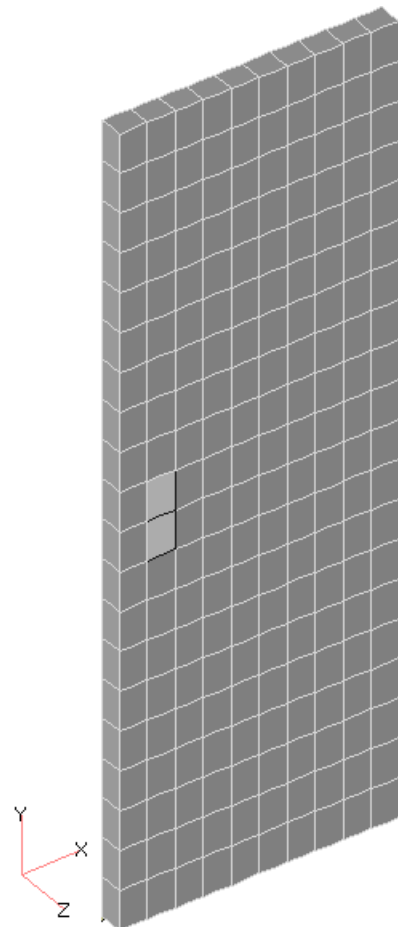
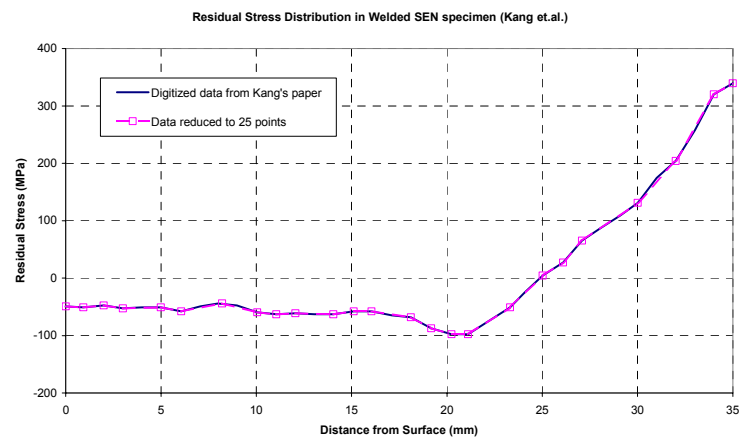


Figure 14 – Effect of start-up with error control stepping



Uncracked mesh with initial crack-block location highlighted



Residual stress distribution

Figure 15 – SEN specimen with residual stress and external cyclic load

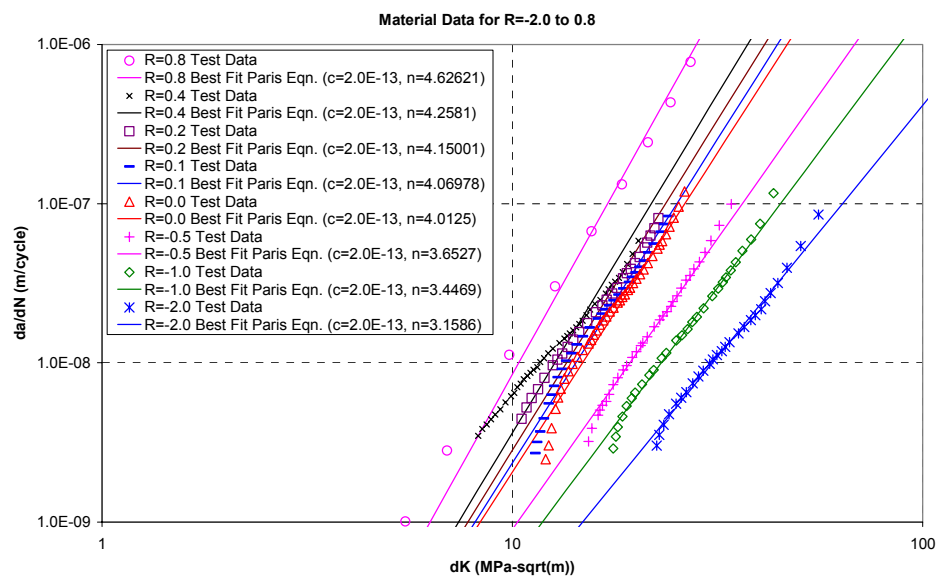


Figure 16 – Crack growth data – Paris lines approximated from actual data

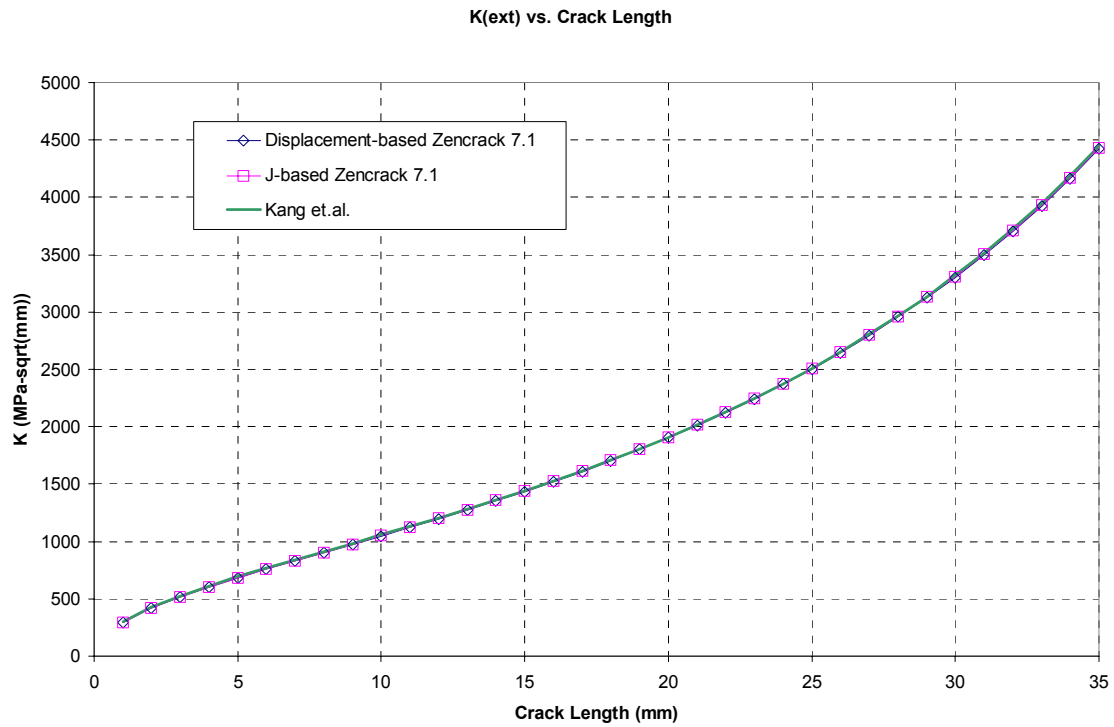


Figure 17 – Mode I stress intensity factor vs crack length for external load

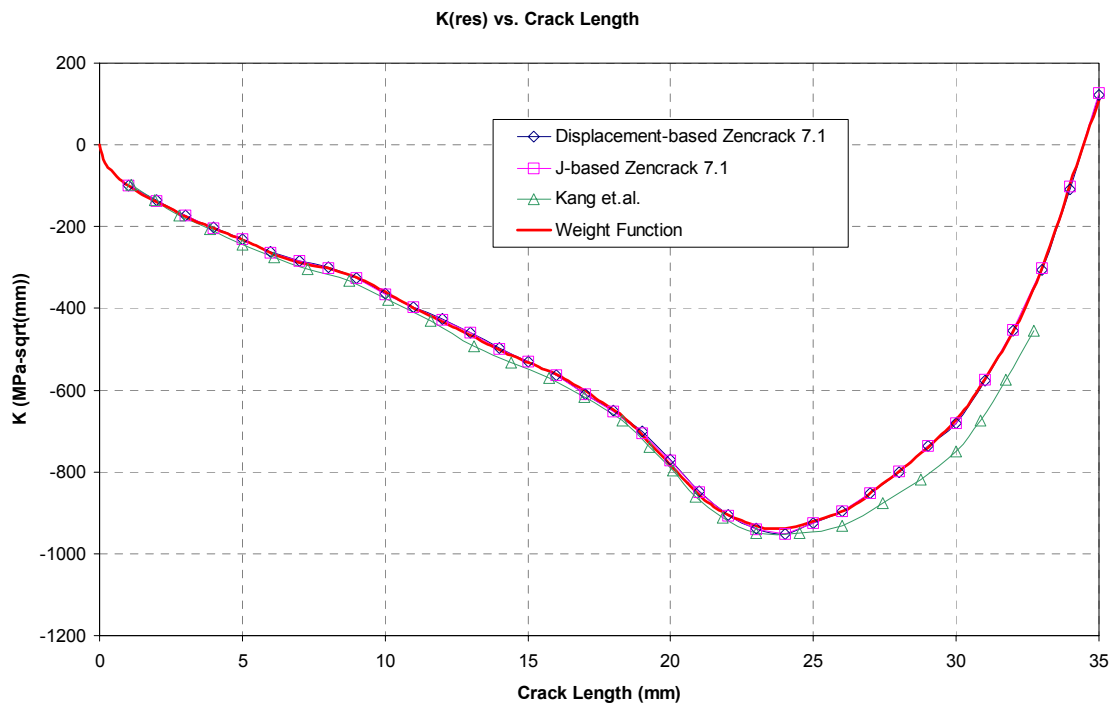


Figure 18 – Mode I stress intensity factor vs crack length for residual stress

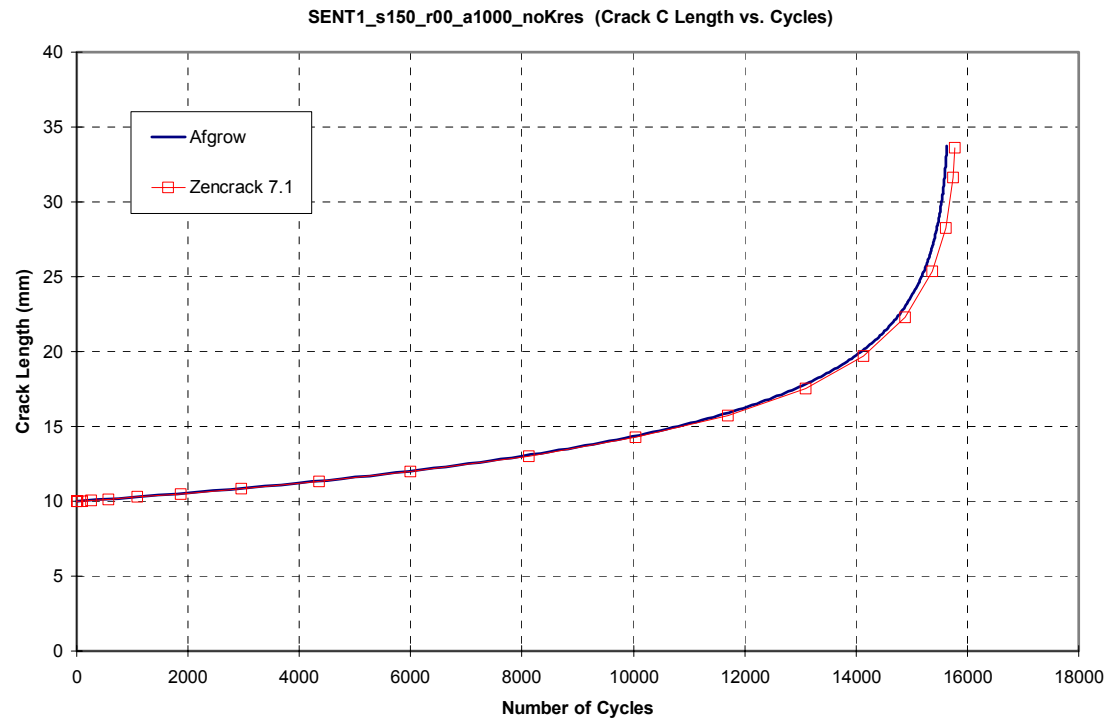


Figure 19 – Crack growth curve for external load without residual stress

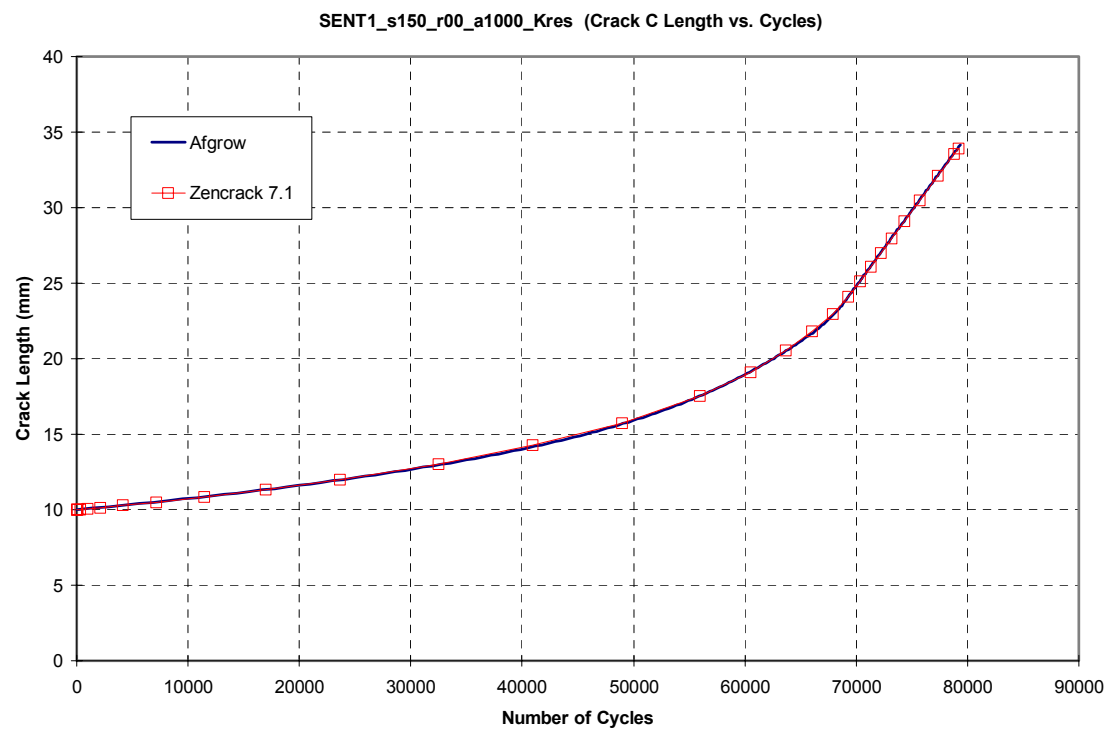


Figure 20 – Crack growth curve for external load plus residual stress

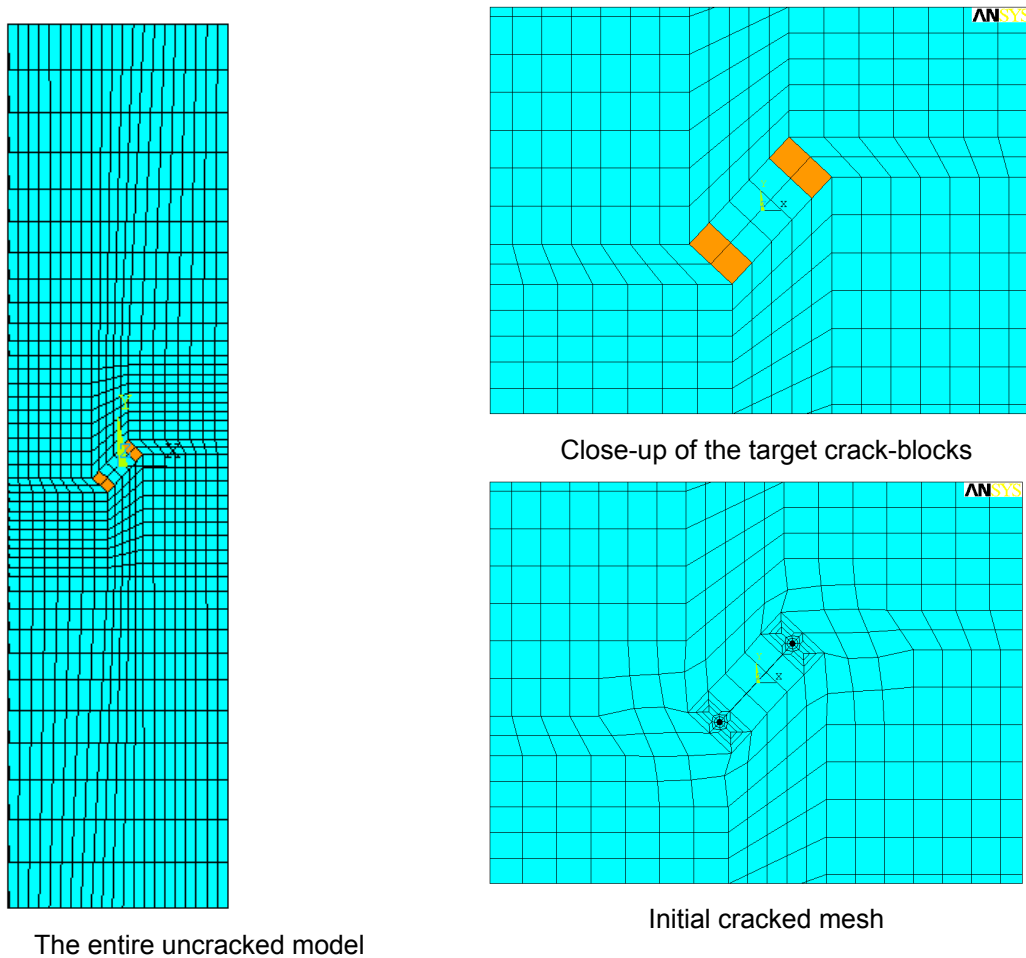


Figure 21 - Mesh for an oblique crack at 43°

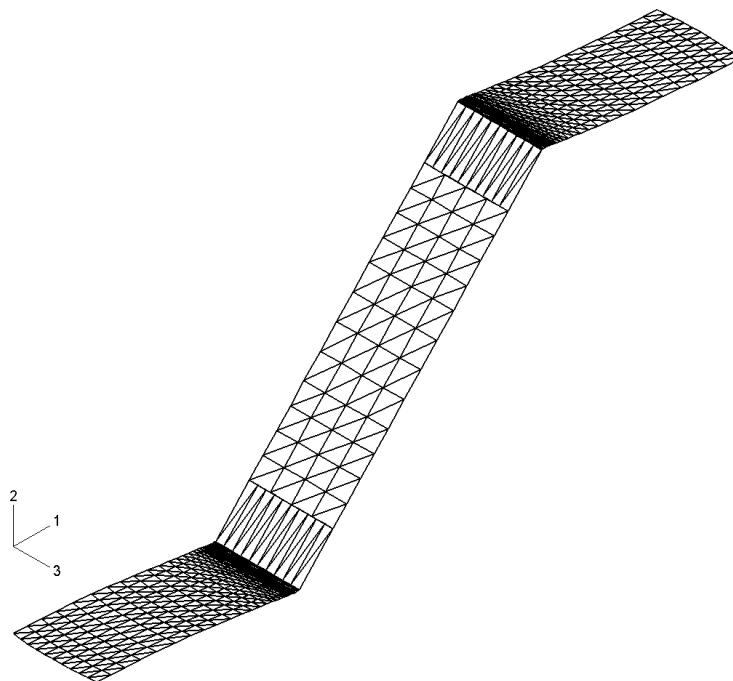


Figure 22 - Crack growth profiles for the oblique crack at 43°

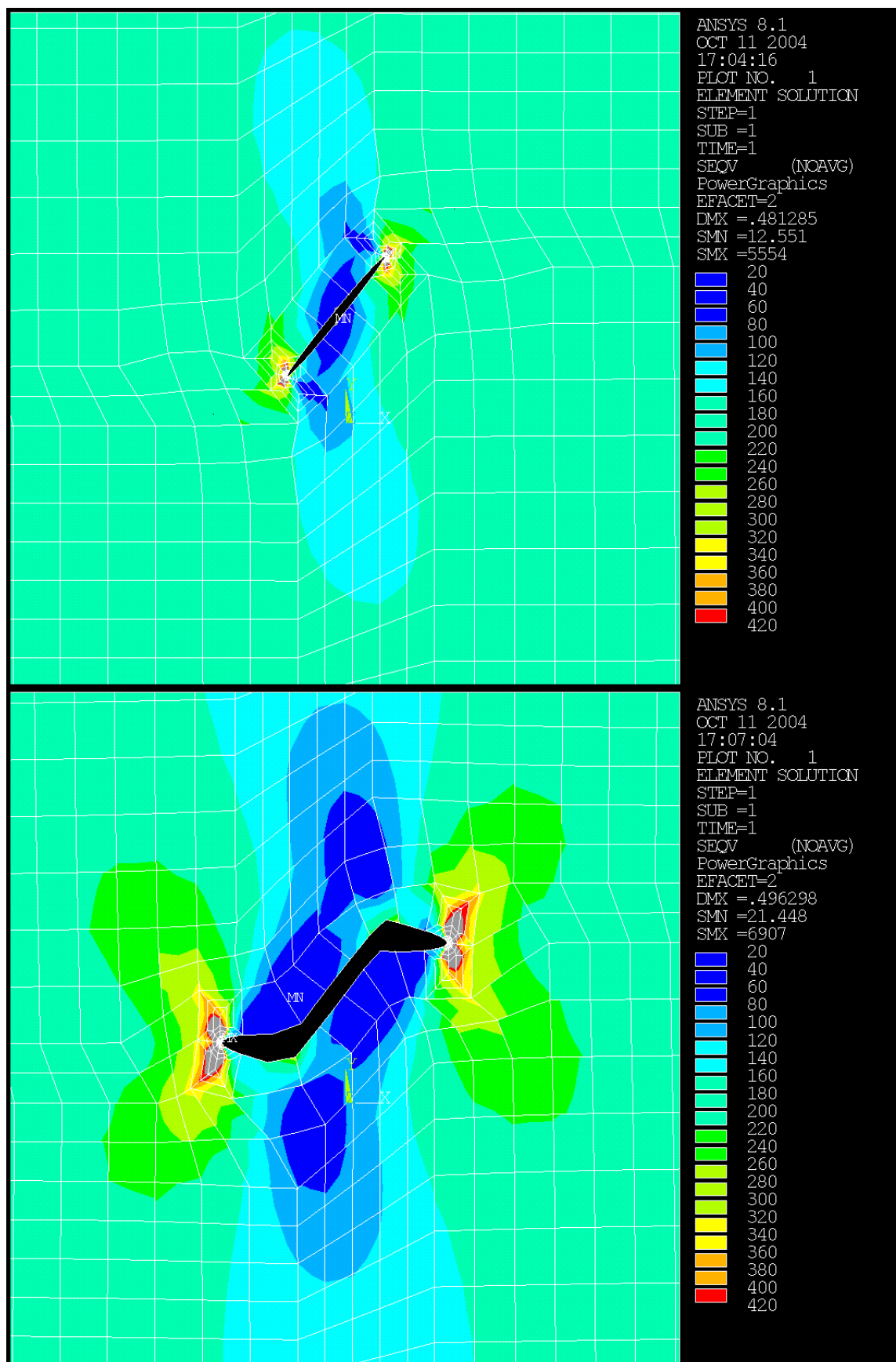


Figure 23 – Mises stress plots at two steps of the simulation

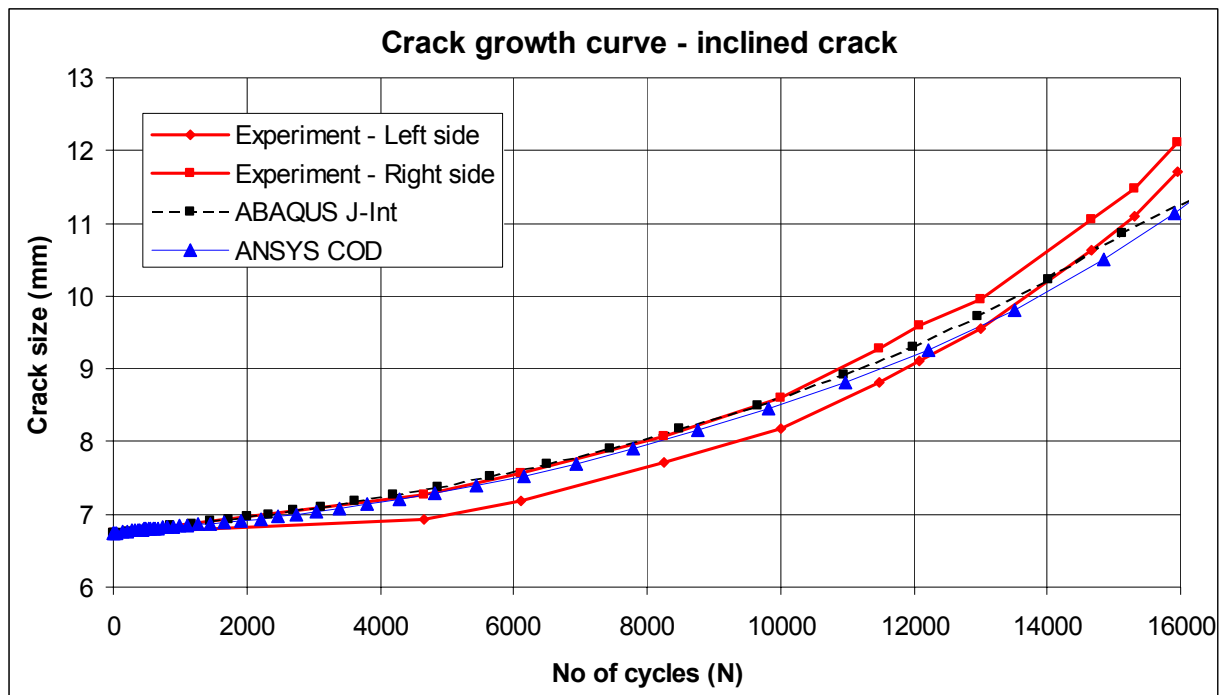


Figure 24 - Crack growth rate for the oblique crack at 43°

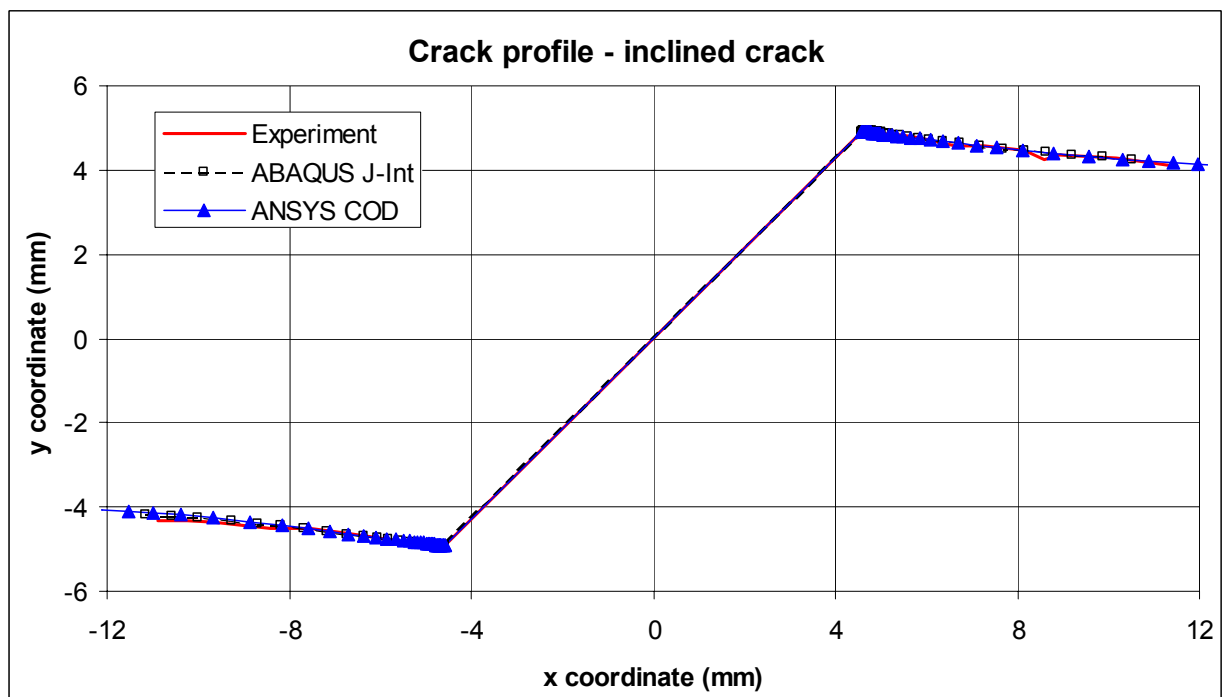
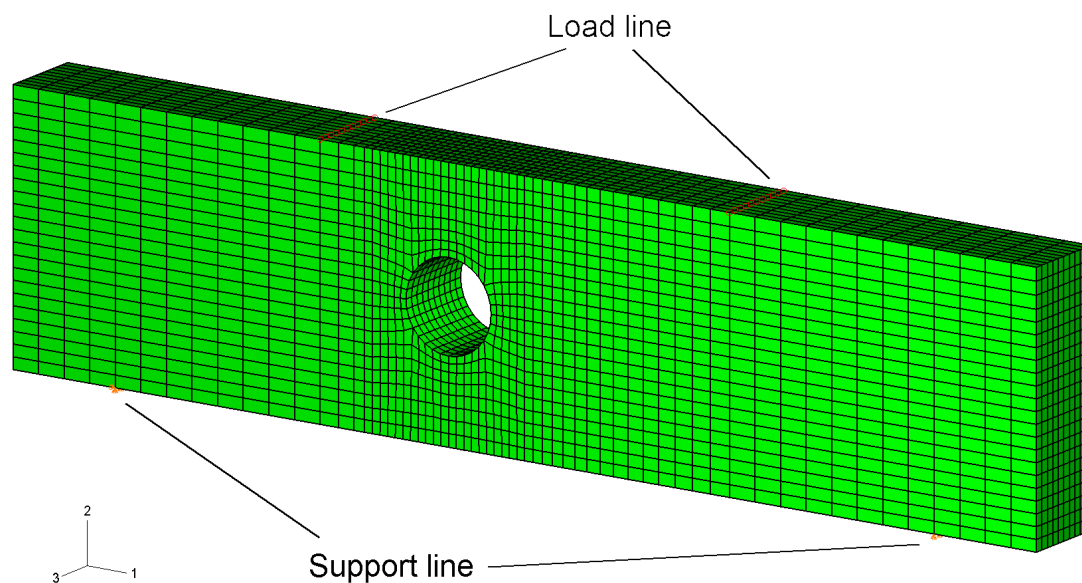
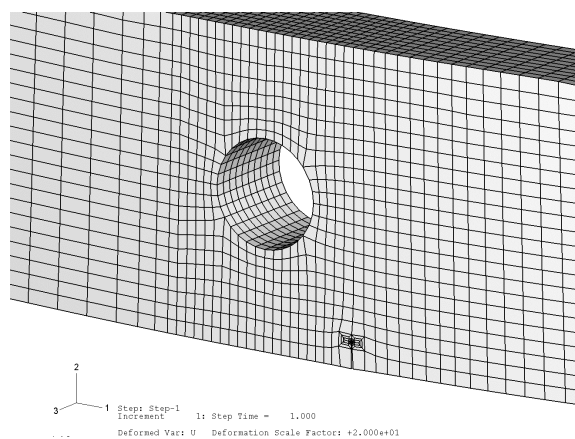


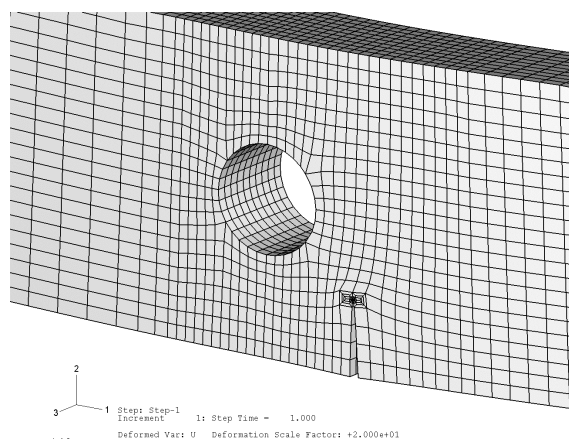
Figure 25 - Comparison of the ZENCRACK and experimental crack growth path for the oblique crack at 43°



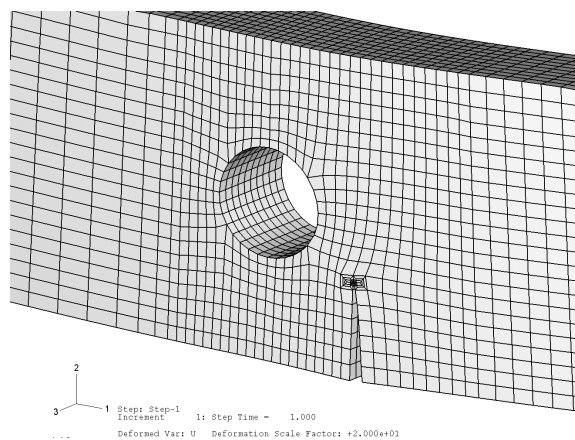
Uncracked mesh for four-point bend specimen with hole showing support and load locations



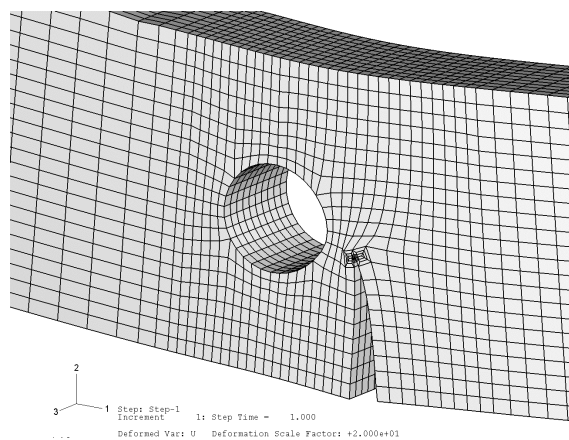
Initial cracked mesh



Mesh 22 of 34

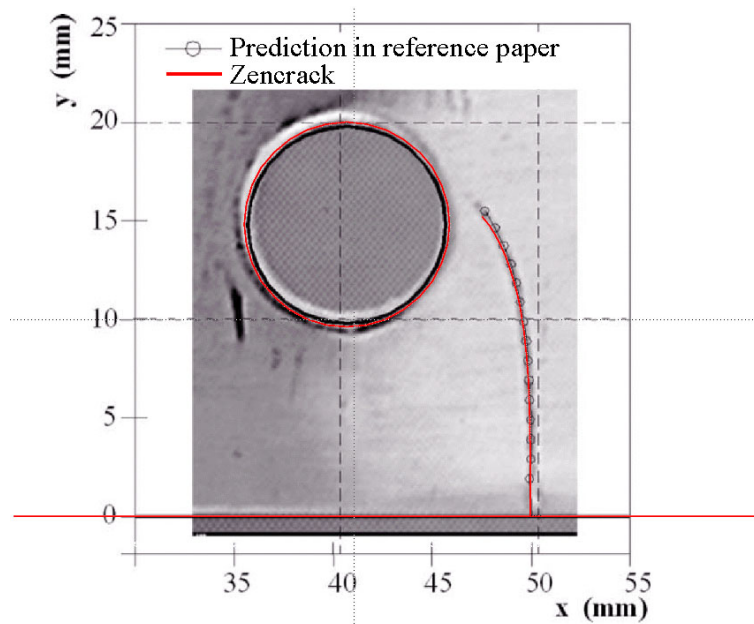


Mesh 25 of 34



Mesh 31 of 34

Figure 26 – SEN specimen with a hole



Comparison between ZENCRACK prediction and reference

Figure 27 – SEN specimen with a hole